Author Manuscript

Author Manuscript

Author Manuscript

Author Manuscript

HHS Public Access

Author manuscript

Glia. Author manuscript; available in PMC 2017 November 01.

Published in final edited form as:

Glia. 2016 November ; 64(11): 1987–2004. doi:10.1002/glia.23037.

Epidermal Growth Factor Preserves Myelin and Promotes Astrogliosis after Intraventricular Hemorrhage

Govindaiah Vinukonda, PhD[1], **Furong Hu**[1], **Rana Mehdizadeh**, **Preeti Dohare, PhD**[1], **Ali Kidwai**[1], **Ankit Juneja**[1], **Vineet Naran**[1], **Maria Kierstead**[1], **Rachit Chawla**[1], **Robert Kayton, PhD**[3], and **Praveen Ballabh, MD**[1,2]

[1]Department of Pediatrics, Maria Fareri Children's Hospital at Westchester Medical Center-New York Medical College, Valhalla, NY 10595

[2]Cell Biology and Anatomy, Maria Fareri Children's Hospital at Westchester Medical Center-New York Medical College, Valhalla, NY 10595

[3]Department of Physiology and Pharmacology, Oregon Health & Science University, Portland, Oregon 97239

Abstract

Intraventricular hemorrhage (IVH) leads to reduced myelination and astrogliosis of the white matter in premature infants. No therapeutic strategy exists to minimize white matter injury in survivors with IVH. Epidermal growth factor (EGF) enhances myelination, astrogliosis, and neurologic recovery in animal models of white matter injury. Here, we hypothesized that recombinant human (rh) EGF treatment would enhance oligodendrocyte precursor cell (OPC) maturation, myelination, and neurological recovery in preterm rabbits with IVH. In addition, rhEGF would promote astrogliosis by inducing astroglial progenitor proliferation and GFAP transcription. We tested these hypotheses in a preterm rabbit model of IVH and evaluated autopsy samples from human preterm infants. We found that EGF and EGFR expression were more abundant in the ganglionic eminence relative to the cortical plate and white matter of human infants and that the development of IVH reduced EGF levels, but not EGFR expression. Accordingly, rhEGF treatment promoted proliferation and maturation of OPCs, preserved myelin in the white matter, and enhanced neurological recovery in rabbits with IVH. rhEGF treatment inhibited Notch signaling, which conceivably contributed to OPC maturation. rhEGF treatment contributed to astrogliosis by increasing astroglial proliferation and upregulating GFAP as well as Sox9 expression. Hence, IVH results in a decline in EGF expression; and rhEGF treatment preserves myelin, restores neurological recovery, and exacerbates astrogliosis by inducing proliferation of astrocytes and enhancing transcription of GFAP and Sox9 in pups with IVH. rhEGF treatment might improve the neurological outcome of premature infants with IVH.

Address for Correspondence: Praveen Ballabh, MD, Regional Neonatal Center, Maria Fareri Children's Hospital at Westchester Medical Center, Valhalla, NY 10595, Pballabh@msn.com, Phone: 914-594-4036, Fax: 914-594-4653.

Author contributions: GV has performed the experiments. PB has designed and the study, and wrote the manuscript. PD, AA, RM, FH, AK, AJ, VR, MK, and RC have performed experiments. RK performed electron microscopy and co-wrote the manuscript.

Conflict of interest: Nothing to report.

Author Manuscript Author Manuscript Author Manuscript Author Manuscript

Keywords

Epidermal growth factor; myelination; astrogliosis; oligodendrocyte progenitor cells; intraventricular hemorrhage; premature infants

Introduction

Intraventricular hemorrhage (IVH) remains a major complication of prematurity that leads to white matter injury (WMI) in premature infants (Ballabh 2014). There is no viable treatment to minimize white matter injury and associated motor and cognitive deficits in the survivors of IVH. Epidermal growth factor (EGF) receptor regulates oligodendrogenesis and promotes myelination in the animal models of neonatal hypoxia-ischemia and lysolechithin-induced demyelination (Galvez-Contreras et al. 2013; Gonzalez-Perez and Alvarez-Buylla 2011). Therefore, we asked whether EGF treatment would restore myelination in rabbit model of IVH and if so, what the underlying mechanisms were.

During intrauterine life, oligodendrocyte progenitor cells (OPCs) are produced initially in the medial ganglionic eminence (GE) and anterior entopeduncular area and later, they are generated in the caudal and lateral ganglionic eminence (Kessaris et al. 2006). EGF and EGF receptor (EGFR) regulate survival, proliferation, and migration of neural precursor cells and induce their differentiation towards oligodendrocyte lineage (Galvez-Contreras et al. 2013; Gonzalez-Perez and Alvarez-Buylla 2011). EGFR overexpression in the ganglionic eminence during early postnatal development increases the population of endogenous stem cells (Type-B cell) and early OPC (Aguirre et al. 2005). In addition, this enhances proliferation of astrocytes and $Dlx2^+$ progenitors in the ganglionic eminences, thereby augmenting gliogenesis at the expense of neurogenesis (Doetsch et al. 2002; Mayer et al. 2009). EGF-induced OPCs are migratory and express nestin, Olig2, and PDGFRα (Gonzalez-Perez et al. 2009). Intriguingly, upon withdrawal of EGF, the OPCs stop migrating and differentiate into myelinating oligodendrocytes in the white matter (Gonzalez-Perez and Alvarez-Buylla 2011). Hence, EGF promotes migration, proliferation, and maturation of OPCs as well as multiplication of astrocytes.

EGF treatment has been demonstrated to offer neuroprotection in both neonatal and adult model of brain injury by stimulating proliferation and maturation of OPCs. Recent studies in a mouse model of neonatal chronic hypoxia have demonstrated that EGF signaling promotes survival, proliferation, and maturation of OPC as well as neurological recovery (Aguirre et al. 2005; Scafidi et al. 2014). In adult models of demyelination, EGF activation enhances proliferation and maturation of OPC resulting in increased myelination and functional recovery (Aguirre et al. 2007; Aguirre et al. 2005). Furthermore, EGF treatment induces recovery in a rat model of traumatic brain injury (Sun et al. 2010). Despite this, the effect of IVH on EGFR pathway in neonatal animal models and therapeutic benefits of EGF treatment in restoring myelination and clinical recovery in an animal model of IVH have remained unexplored.

EGF signaling is mediated by several pathways, including Akt, MAP kinase, and JAK/STAT pathways (Jorissen et al. 2003). Akt is a serine/threonine kinase which regulates cell

Author Manuscript Author Manuscript Author Manuscript Author Manuscript

survival, proliferation, and maturation. In oligodendrocyte, it specifically enhances production of myelin via mammalian target of rapamycin (mTOR) signaling (Flores et al. 2008). Activation of STAT-3 specially promotes astrogliogenesis and suppresses neurogenesis (Herrmann et al. 2008). A switch from neurogenesis to gliogenesis is in progress in late pregnancy, which is initiated and driven by NFIA and Sox9 transcription factors (Kang et al. 2012; Molofsky and Deneen 2015). As astrocytes mature, they express several markers, including GFAP, vimentin, S-100β, and others. GFAP promotor in astrocytes is regulated by several factors, including Notch, bone morphogenetic protein, leukemia inhibiting factor, and others (Herrmann et al. 2008; Molofsky and Deneen 2015), which might be affected by the development of IVH and EGF treatment. EGF is known to enhance proliferation of astrocytes and convert quiescent astrocytes into reactive astrocytes (Liu et al. 2006; Liu and Neufeld 2007; Mayer et al. 2009). However, the effect of EGF on OPC and astrocytes in infants or animal models of IVH has not been studied.

Based on these considerations, we hypothesized that EGF treatment would promote OPC proliferation and differentiation, myelination, and clinical recovery in rabbit pups with IVH, which might be mediated by Akt-mTOR signaling. We also postulated that rhEGF would promote astrogliosis by driving astrocyte proliferation, enhancing GFAP, and inducing NFIA and Sox9 transcription factors.

Material and methods

Animals

The Institutional Animal Care and Use Committee of the New York Medical College, Valhalla, NY approved the present study. We used our preterm rabbit model of glycerol-induced IVH for this study (Chua et al. 2009; Dummula et al. 2011; Vinukonda et al. 2010). Briefly, we purchased timed-pregnant New Zealand white rabbits from Charles River Laboratories, Inc. (Wilmington, MA). We performed C-section to deliver the premature pups at E29 (full-term=32 days). Newborn pups were reared in an infant incubator at a temperature of 35° C. We used puppy formula (Zoologic, Petag, IL) to gavage-feed the pups in a volume of ~2 ml every 12 h (100 ml/kg/day) for the first 2 days, and feeds were advanced to 125, 150, 200, 250 and 280 ml/kg at postnatal days 3, 5, 7, 10 and 14, respectively. We treated rabbit pups of either sex with 50% intraperitoneal glycerol (6.5 gm/kg) at 2 h of age to induce IVH. Severity of IVH was determined by measuring ventricle volume (length, breadth & depth in coronal & sagittal views) on head ultrasound at 24 h age using an Acuson Sequoia C256 (Siemens) ultrasound machine. Pups were classified as moderate (30–150 mm^3) and severe (151–250 mm^3) IVH, based on ventricular volume. Ventricular volume <30 mm^3 indicated microscopic or no IVH. The pups with moderate and severe IVH were assigned into treatment and control groups so that the severity of IVH was balanced between the comparison groups.

Recombinant human EGF (rhEGF) treatment

The rabbit pups with IVH were sequentially treated with either 5 μl of recombinant human epidermal growth factor (Millipore Billerica, MA, USA; 250 ng per dose each lateral ventricle) or vehicle at days 2 (24 h age), 4 and 6 intracerebroventricularly on both sides.

Author Manuscript Author Manuscript Author Manuscript Author Manuscript

Briefly, the pups were mounted on a rabbit pup restrainer after anesthetizing them with ketamine and xylazine. A needle of 28 gauge with 10 μl Hamilton syringe was mounted on a micromanipulator to inject the EGF into the ventricle. We used the following coordinates from bregma: 1 mm anterior, 4 mm lateral, and 3 mm deep. The dose of EGF was calculated based on its previous use in rats (Kuhn et al. 1997; Sun et al. 2010). The severity of IVH, measured by ultrasound, was similar between the comparison groups—vehicle treated pups with IVH and rhEGF-treated pups with IVH.

Human subjects

The Research Administration of New York Medical College, Valhalla, NY approved the use of autopsy brain samples from premature infants to conduct this study. The postmortem materials included forebrain tissue samples taken at the level of the head of caudate nucleus from premature infants with and without IVH of 23–27 gestational weeks (gw) and less than 5 days of postnatal age. Samples were obtained less than 18 h postmortem. We excluded premature infants with hypoxic-ischemic encephalopathy, meningitis, culture proven sepsis, major brain or spinal cord malformation, chromosomal defects, and history of neurogenetic disorders. We included 6 infants from each of the two groups, including IVH (grade 3 or 4) and no IVH. The wall of the cerebral hemisphere in premature infants consists of ventricular zone (VZ), subventricular zone (SVZ), intermediate zone, cortical plate, and marginal zone as illustrated by the Boulder Committee (Bystron et al. 2008). In the present study, we described intermediate zone embryonic white matter synonymously with white matter, and cerebral cortex for the cortical plate.

Rabbit tissue collection and processing

We processed the tissues as previously described (Ballabh et al. 2007). The brain slices were immersed in 4% paraformaldehyde in phosphate buffered saline (PBS; 0.1 M, pH 7.4) for 18 hours and then were cryoprotected by keeping them into 15% sucrose in 0.1 M PBS buffer for 24 h followed by 30% sucrose for the next 24 h. We next froze the tissue slice after embedding into optimum cutting temperature compound (Sakura, Japan). Frozen coronal blocks were cut on a cryostat into coronal sections of 20 μm thickness. For Western blot analyses, coronal slices of 1–2 mm thickness were harvested at the level of the midseptal nucleus of the forebrain and snap frozen on dry ice.

Human tissue collection and processing

We processed the human tissues as in our prior studies (Ballabh et al. 2007). About 3–4 mm thick coronal slices were cut at the level of head of caudate nucleus from the fronto-parietal lobe. The coronal blocks comprised cortical plate, embryonic white matter, and ganglionic eminence. The samples were immersion-fixed in 4% paraformaldehyde in PBS for 18 h and were then cryoprotected by immersion into a 15% sucrose solution in PBS, followed by 30% sucrose in PBS. The tissues next were frozen after embedding them into optimum cutting temperature compound (Sakura, Japan). Frozen coronal blocks were cut into 20 μm thick sections. For Western blot analyses, pieces of tissues were directly harvested from the cortex, white matter, and ganglionic eminence and snap frozen on dry ice.

Author Manuscript Author Manuscript Author Manuscript Author Manuscript

Immunohistochemistry

Immunohistochemical staining was performed as described previously (Ballabh et al. 2007). The primary antibodies used in experiments included: rabbit epidermal growth factor (catalog #06-102, Millipore, Billerica, MA, USA), mouse epidermal growth factor receptor (Catalog # 2232, Cell signaling technology, Danvers, MA), goat polyclonal Ki67 (catalog #275R-14, Cell Marque, Rocklin, CA), goat polyclonal Olig2 (catalog #AF-2418, R&D, Minneapolis, MN), mouse monoclonal GFAP (catalog #G6171, Sigma-Aldrich, St. Louis, MO), rat monoclonal myelin basic protein (MBP; catalog #AB7439, Abcam, Cambridge, MA), goat polyclonal PDGFRα (catalog #AR307, R & D, Minneapolis, MN), mouse monoclonal myelin associated glycoprotein (MAG; catalog #AB89780, Abcam, Cambridge, MA), biotinylated O4 monoclonal antibody (provided by Dr. Rashmi Bansal, University of Connecticut), and mouse monoclonal Nkx2.2 (Hybridoma Bank, University of Iowa, IA). Secondary antibodies used were Cy-3 conjugate donkey anti-mouse, Cy-3 conjugate donkey anti-goat, and FITC conjugate donkey anti-rat (Jackson Immunoresearch, West Grove, PA). Briefly, we hydrated the fixed sections in 0.01 M PBS, blocked the sections with normal donkey serum in PBS with 0.01% Triton-X (PBST), and incubated with the primary antibodies diluted in PBST at 4° C overnight. After several washes in PBS, the sections were incubated with secondary antibody diluted in 1% normal goat serum in PBS at room temperature for 60 min. Finally, after washing in PBS, sections were mounted with Slow Fade Light Antifade reagent (Molecular Probes, Invitrogen, CA) and were visualized under a confocal microscope (Nikon Instruments, Japan). Stereology was performed using a fluorescent microscope (Axioskop 2 plus, Carl Zeiss Inc) with motorized specimen stage for automated sampling (ASI, Eugene, OR), with a CCD color video camera (Microfire; Optronics, Goleta, CA) and stereology software (Stereologer, SRC, Baltimore, MD).

Quantification of oligodendrocytes

Proliferation and maturation of OPC were assessed in the corona radiata and corpus collosum of pups without IVH and pups with IVH treated with vehicle or rhEGF. We injected intramuscular BrdU in these three sets of animals in a dose of 50 mg/kg twice a day for two days and animal were euthanized at D3. Cycling OPCs (S-phase of cell cycle) were identified by double-labeling the coronal sections with BrdU and Olig2 or PDGFRα antibodies, while maturation of OPC was evaluated by double-labeling the sections with Olig2 and Nkx2.2 antibodies. All coronal sections were obtained at the level of the midseptal nucleus (five 20 μm sections at an interval of 90 μm). Quantification was performed by a blinded investigator in a random and unbiased fashion using a confocal microscope with a 60× lens (Nikon Instruments, Japan). Cells were counted in ~25 images (5 images × 4–5 sections) for each brain region for every parameter for each pup (n=5 pups per group).

Stereological assessment of myelin and astrocytes in the corona radiate and corpus callosum

We quantified several stereological parameters using computerized software system (*Stereologer,* Stereology Resource Center, Chester, MD). Briefly, coronal sections of 30 μm thickness were cut on a cryostat with a section sampling interval of 90 μm to accomplish 6

Author Manuscript Author Manuscript Author Manuscript Author Manuscript

sections or more at the level of mid-septal nucleus. The sections were double-labeled with myelin basic protein (MBP) antibody and DAPI (nuclear stain) and quantified as follows. The reference spaces (corona radiata, corpus callosum) were marked on the section under a 5× objective. The volume of the outlined area (reference space) was quantified using a point counting probe (frame 25 μm × 25 μm; guard zone 2 μm, inter-frame interval = 300 μm). The total volume fraction (load) of myelin stained by MBP antibody through a defined reference space was quantified using the object area fraction probe under 60× oil lens. For the area fraction probe (frame 25 μm × 25 μm; guard zone 2 μm, interframe interval 400 μm), the investigator clicked on the grid points that overlapped the myelin fibers in sections labeled with MBP. The area fraction of myelin was estimated as the ratio of product of the area per point and the number of points hitting the reference area [a(point)$^{\bullet}\Sigma P_{ref}$] over the product of the area per point and number of points hitting the sampled area [a(point)$^{\bullet}\Sigma P_{samp}$], as reported previously.(Mouton et al. 2009) A coefficient of error (CE) < 0.10 was acceptable. To assess astrogliosis, we quantified total volume fractions of astrocyte cell bodies and glial fibers in a similar manner as for myelin (Mouton et al. 2009).

Western blot analyses

We homogenized the frozen brain tissue in sample buffer (3% SDS, 10% glycerol and 62.5 mM Tris-HCl) by mechanical homogenizer and then sonicated the lysate before centrifugation. We measured supernatant protein concentrations using a BCA protein assay kit (Pierce Kit #23227, Thermo Scientific, Rockford, IL) with BSA to create the standard curve. After boiling the samples in Laemmli buffer (catalog #161-0737, BioRad, CA), total protein samples were separated by SDS-PAGE.(Ballabh et al. 2007) Equal amounts of protein (10–20 μg) were loaded onto 4–15% or 4–20% gradient precast gels (BioRad, CA), based on the molecular weight of the target protein. Separated proteins were transferred onto polyvinylidene difluoride (PVDF) membranes by electro-transfer. We next incubated the membranes overnight with primary antibodies. We detected target proteins with chemiluminescence ECL system (GE Healthcare) by using secondary antibodies conjugated with horseradish peroxidase (Jackson Immunoresearch, West Grove, PA). We then stripped the blots using stripping buffer (2.5% SDS, 0.7% 2-mercaptoethanol, 62.5 mM Tris-HCl, pH 6.8) and incubated with β-actin antibody (catalog #A5316, Sigma, St. Louis, MO) followed by secondary antibody and detection with chemiluminescence ECL system. As described previously,(Vinukonda et al. 2010) the blots from each experiment were densitometrically analyzed using Image J. Optical density (OD) values were normalized to β-actin. Antibodies used for Western blot analyses were the same as used for immunohistochemistry. In addition, we used mouse monoclonal vimentin (Hybridoma Bank, University of Iowa, IA), mouse monoclonal STAT3 (Cell signaling technology, Danvers, MA), rabbit polyclonal P-STAT3 (Tyro705, Cell signaling technology, Danvers, MA), mouse monoclonal Akt (BD biosciences, San Jose, CA), mouse monoclonal P-Akt (BD Bioscience, San Jose, CA), rabbit polyclonal mTOR (Cell Signaling Inc., Danvers, MA), rabbit polyclonal P-mTOR (Cell Signaling Inc., Danvers, MA), mouse monoclonal beta actin (Sigma-Aldrich), rabbit polyclonal NFIA (Active Motif, Carlsbad, CA), rabbit polyclonal Sox9 (Millipore, Billerica, MA), NICD (R & D Systems, Minneapolis, MN), mouse monoclonal Hes5 (Sigma-Aldrich), mouse monoclonal Dlx1 (NIH Neuromab, UC Davis, CA), and Mash1 (BD Biosciences, San Jose, CA) primary antibodies..

Author Manuscript Author Manuscript Author Manuscript Author Manuscript

Quantitative Real-Time Polymerase Chain Reaction (qRT-PCR)

Gene expression was performed by real time PCR as previously described (Ballabh et al. 2007). Briefly, total RNA was isolated using a RNeasy Mini kit (catalog #74104, Qiagen) from a coronal brain slice taken at the level of the mid-septal nucleus. cDNA was synthesized using Superscript II RT enzyme (catalog # 05081955001, Roche, Indianapolis, IN) followed by real time quantitation using SYBR green (catalog # 04913850001, Roche, Indianapolis, IN) with an ABI Prism 7900HT Sequence Detection System (Applied Biosystems). Analysis was completed using the efficiency corrected ΔΔCT method. The following primers were used: GFAP (accession number: NG_008401) sense: ACTCAATGCTGGCTTCAAGGAGAC, antisense: ATGTAGCTGGCAAAGCGGTCATTG. The gene expression for EGFR1 (Assay ID: OC 33955872_g1), EGFR2 (Assay ID: OC04096730_m1), EGFR3 (Assay ID:OC03395874_m1), EGFR4 (Assay ID: OC 03395876_m1), Sox9 (Assay ID: Oc04096872_m1), NFIA (Assay ID: Hs00325656_m1) were assayed using primers plus MGB TaqMan probes from Life Technologies (Norwalk, CT).

Electron microscopy

We processed brains (14 d) from glycerol treated pups without IVH, pups with IVH, and rhEGF treated pups with IVH (n = 3–4 each). We took slices (2 mm thickness) from freshly harvested rabbit pup brain using a brain slicer matrix and then dissected corona radiata and corpus callosum in a petri dish under a SteReo discovery microscope (Carl Zeiss). The dissected tissues of the white matter were fixed into 2.5% glutaraldehyde overnight. The tissues were then washed in 0.1 M sodium cacodylate buffer, pH 7.4, postfixed in buffered osmium tetroxide for 1–2 h, stained *en bloc* with 1% uranyl acetate, dehydrated in graded ethanol solutions, and embedded in epoxy resin. We next placed sections of 60–90 nm thicknesses onto 200 mesh grids, stained with uranyl acetate and lead citrate, and then the sections were examined with a Techni 12 electron microscope at 80 Kv. Digital images were acquired using a 16 megapixel Advanced Microscopy Techniques camera. We acquired 12–20 images per brain. Electron micrographs were assessed for myelinated axons per unit area; and the g-ratio (ratio of axonal diameter with myelin sheath and axonal diameter without myelin sheath) of myelinated axons in the 3 groups of pups were calculated using Image J (NIH).

Statistics and Analysis

Data are expressed as means ± standard error of the mean (s.e.m.). To determine differences in the myelin basic protein (MBP), myelin associated glycoprotein (MAG), GFAP, vimentin, STAT-3, mTOR, and Akt on Western blot analyses and cell counts between 3 groups (no IVH, vehicle- and rhEGF-treated kits), we used one way ANOVA. Gene expressions for EGFR1–4, EGF, NFIA, Sox9, vimentin and GFAP between the three groups at day 3 and 7 were compared by employing two-way ANOVA. To compare EGF and EGFR expression, in the three brain regions between infants with and without IVH, we employed two-way ANOVA with repeated measures. All post hoc comparisons were done by Tukey multiple comparison test at the 0.05 significance level.

Author Manuscript Author Manuscript Author Manuscript Author Manuscript

RESULTS

EGFR is enriched in the GE of human preterm infants and does not change with development of IVH

To compare EGFR expression between premature human infants with and without IVH (23–27 gestational weeks), we labeled coronal sections from the forebrain with EGFR specific antibody. We found that EGFR was abundantly expressed in the medial and lateral GE (colloquially known as germinal matrix) and weakly in the cortical plate, dorsal cortical subventricular zone (SVZ), and embryonic white matter. Double labeling of EGFR with GFAP, Olig2, and nestin specific antibodies revealed that EGFR was predominantly expressed on the $Olig2^+$ and $nestin^+$ precursor cells of ventricular zone and SVZ in the GE as well as the white matter (Fig. 1A). Moreover, EGFR expression was weak on the $GFAP^+$ glial cells in almost all the cortical compartments. Western blot analyses on homogenates made from tissues harvested from these regions confirmed that EGFR expression was significantly higher in the GE compared with the cortical plate or white matter in infants with IVH (P= 0.001 and 0.004, Fig. 1B). Moreover, EGFR expression was also elevated in the GE relative to the white matter in pups without IVH (P=0.038). Importantly, EGFR levels were comparable between infants with and without IVH in all the three regions (Fig. 1B). Weak-to-absent expression of EGFR on the $GFAP^+$ astroglial cells has also been reported in adult astrocytes (Liu and Neufeld 2007).

We next evaluated preterm rabbit forebrains (E29) for the expression of EGFR. Western blot analyses showed that there was no difference in EGFR expression between rabbits with and without IVH at both postnatal 48 and 72 h after the induction of IVH (Fig. 1B). Real time qPCR using taqman probes (Life Tech, Norwalk, CT) also showed comparable mRNA expression of EGFR1–4 in pups with and without IVH at both postnatal days (D) 3 and 7 (data not shown). A satisfactory immunolabeling could not be obtained with the commercially available EGFR antibodies in the rabbit brain sections. Together, EGFR is more abundantly expressed in the GE relative to the white matter and cortical plate; and IVH does not affect its expression.

EGF expression is reduced in both rabbits and humans with IVH

To evaluate EGF expression in the GE, white matter, and cortical plate of preterm human infants with and without IVH, we immunostained forebrain sections with EGF specific antibody. We found that EGF expression was more abundant in the GE relative to the white matter and cortical plate of infants without IVH (Fig. 2A). Moreover EGF immunoreactivity was reduced in the GE of infants with IVH compared to infants without IVH, however EGF expression in the cortical plate and embryonic white matter was comparable between infants with and without IVH. Double immunolabeling of the forebrain sections with EGF and neural cell markers—GFAP, Olig2, and nestin—revealed that EGF was expressed abundantly on $GFAP^+$ and $nestin^+$ radial glial cells of the GE and the dorsal cortical SVZ (Fig. 2A; Data on cortical SVZ not shown). However, EGF expression was weak-to-absent on $Olig2^+$ OPCs. Quantification of EGF protein (15 kDa) by Western blot analyses confirmed that EGF expression was higher in GE relative to the cortex and white matter of infants without IVH (P=0.002, 0.004), but not of infants with IVH (Fig. 2B). More

Author Manuscript Author Manuscript Author Manuscript Author Manuscript

importantly, EGF (15 kDa) levels were reduced in the GE of infants with IVH compared to controls without IVH (P=0.019), but not in the cortex or white matter.

We next assessed EGF expression in the preterm rabbits with and without IVH. Western blot analyses showed that EGF (15 kDa) protein expression was reduced in the forebrain of rabbits with IVH compared with untreated and glycerol-treated controls without IVH at postnatal 48 h (P=0.034 and 0.003), but not at 72 h (Fig. 2B). In contrast to protein expression, EGF mRNA expression, which was measured by real time PCR, was comparable between rabbits with and without IVH (data not shown). We might attribute this difference between protein and gene expression of EGF to rapid mRNA turnover. Collectively, EGF expression is higher in periventricular GE relative to the white matter and cortex in infants without IVH and the development of IVH reduces EGF expression in both rabbits and humans.

Human recombinant EGF protein preserved myelin in rabbits with IVH

Since EGF treatment promotes myelination in both neonatal model of chronic hypoxia and adult models of demyelination, we postulated that treatment with human recombinant (rh) EGF would restore myelination in preterm rabbit pups with IVH compared to vehicle controls. To this end, we compared three sets of rabbit pups at D 14: a) glycerol-treated pups without IVH, b) vehicle-treated pups with IVH, and c) rhEGF-treated pups with IVH. To clarify, all pups with IVH received glycerol to induce IVH, and then they alternatively received either rhEGF or vehicle. Severity of IVH (Fig. 3A) was similar between vehicle and rhEGF-treated groups, as measured by head ultrasound. We performed immunolabeling and stereological quantification of myelin in brain sections labeled with myelin basic protein (MBP) antibody. Our analyses demonstrated that the volume fractions (myelin load) of MBP in the corpus callosum and corona radiata were significantly reduced in pups with IVH relative to controls without IVH ($P<0.023$) and that ICV rhEGF injection restored the expression of MBP ($P = 0.013$, Fig. 3B). Accordingly, Western blot analyses confirmed that MBP levels were diminished in pups with IVH compared to glycerol-treated and untreated (no glycerol) controls without IVH ($P < 0.001$ both, Fig. 3C) and that rhEGF treatment significantly increased MBP expression in pups with IVH ($P = 0.001$). Similarly, MAG levels, assayed by Western blot analyses, were significantly higher in rhEGF-treated pups compared with vehicle controls with IVH ($P = 0.001$, Fig. 3C).

To assess morphology and density of myelinated axons in rhEGF treated pups with IVH compared to vehicle-treated pups with IVH and glycerol controls without IVH, we evaluated myelin ultrastructure in the three sets of pups at D 14 (Fig. 3D). We found that the density of myelinated axons were less in pups with IVH compared to controls without IVH ($P < 0.004$) and that rhEGF treatment significantly increased the number of myelinated axons in pups with IVH ($P < 0.027$). Moreover, the g-ratio was similar in the three groups of pups (0.767 ± 0.011 vs. 0.763 ± 0.002 vs. 0.78 ± 0.017, in pups without IVH, with IVH and EGF treatment, respectively). This suggests that rhEGF treatment preserves myelin in rabbits with IVH.

Author Manuscript Author Manuscript Author Manuscript Author Manuscript

rhEGF administration restores neurological recovery

To determine whether rhEGF treatment enhances neurological recovery in rabbit pups with IVH, we performed neurobehavioral scoring on the three sets of preterm pups at D14 (Table), as described before (Dummula et al. 2011; Vinukonda et al. 2010). We noted significant weakness in the right hind leg of two pups, both hind legs of one pup, and right arm of one pup in the vehicle treated controls with IVH. However, only one pup in the rhEGF treated group displayed left hind-leg weakness. The average distance traveled in one minute was higher in rhEGF treated pups compared to vehicle controls (P=0.037). The scores for gait were significantly better in rhEGF treated pups relative to controls. Percentage of pups showing inability to hold their position on a ramp pitched at 60° inclination for 15 seconds or longer was more in rhEGF-treated pups compared to saline controls (40% vs. 11%). Moreover, scores for righting reflex and gait was superior in the treatment group compared to vehicle controls (P<0.05). We did not find any abnormal behavior in the rhEGF treated pups, which we can be attributed to rhEGF administration. There was no difference in sensory and cranial nerve evaluation of the three sets of rabbit pups.

rhEGF treatment enhances both proliferation and maturation of OPC

Since rhEGF preserved myelin in glycerol model of IVH and as rhEGF induces proliferation and maturation of OPC in a model of chronic hypoxia (Aguirre et al. 2005; Scafidi et al. 2014), we postulated that rhEGF treatment might enhance proliferation and maturation of OPCs. To this end, we compared cycling and total number of OPCs in glycerol-treated pups without IVH, vehicle-treated, and rhEGF-treated pups with IVH. All the three groups of animals were treated with intramuscular BrdU, and OPCs were labeled with BrdU and PDGFRα or Olig2 specific antibodies (Fig. 4A, 4B). The densities of both total and proliferating (S-phase of the cell cycle) PDGFRα$^+$ cells were reduced in vehicle-treated pups with IVH compared to controls without IVH at D3 (P = 0.041, 0.034, respectively). More importantly, rhEGF treatment elevated the densities of both total and proliferating PDGFRα$^+$ cells compared to the vehicle controls at D3. (P = 0.022, 0.001, respectively, Fig. 4A). Similar to PDGFRα, both total and proliferating Olig2$^+$ cells showed a trend toward decline in pups with IVH compared to controls without IVH and rhEGF treatment increased the density of total Olig2$^+$ cells (P=0.017, Fig. 4B), but not of Brdu$^+$Olig2$^+$ cells.

We next evaluated the effect of rhEGF treatment on OPC maturation in sections double labeled with Olig2 and Nkx2.2 specific antibodies. We chose Nkx2.2 antigen on OPCs to assess maturation because it is expressed on myelinating (immature OPC) OPCs. We found that population of Olig2$^+$Nkx2.2$^+$ cells was significantly reduced in pups with IVH relative to controls without IVH (P<0.001), and rhEGF treatment significantly increased their density (P = 0.002) in both corona radiata and corpus callosum (Fig. 4C). This suggests that rhEGF treatment promotes the maturation of OPCs in pups with IVH. Consistent with this conclusion, we found higher levels of CNPase (2′,3′-cyclic nucleotide-3′-phosphodiesterase), as measured by Western blot analyses, in rhEGF treated pups with IVH compared to vehicle controls (P<0.035, data not shown) at D14. Together, rhEGF treatment promotes both proliferation and maturation of OPCs.

Author Manuscript Author Manuscript Author Manuscript Author Manuscript

rhEGF treatment does not affect Akt and mTOR pathways in rabbits with IVH

Akt-mTOR signaling promotes CNS myelination through mTOR pathway in mouse models (Flores et al. 2008; Guardiola-Diaz et al. 2012; Narayanan et al. 2009; Tyler et al. 2011). Conversely, STAT-3 signaling inhibits myelination by diverting differentiation of OPC lineage into astrocytes in model of murine encephalomyelitis (Sun et al. 2015). Therefore, we evaluated Akt, mTOR and STAT-3 signaling pathways in rhEGF treated rabbits with IVH compared to the respective controls at both D3 and 7. We found that total-Akt, P-Akt, total mTOR, and P-mTOR expression were comparable between controls without IVH, vehicle- and rhEGF treated pups with IVH (Fig 5A, 5B, data for D3 not shown).

We next evaluated the effect of rhEGF treatment on STAT-3 signaling pathways. Total STAT3 levels were comparable between IVH, vehicle- and rhEGF treated pups with IVH. However, P-STAT3 (Tyr 705) levels were higher in pups with IVH compared to controls without IVH and rhEGF treatment did not affect the expression of P-STAT-3 (Fig. 5C). The data suggest that the development of IVH does not affect Akt and mTOR pathways, but activates STAT3 pathway. More importantly, rhEGF treatment does not activate any of these pathways in pups with IVH.

rhEGF treatment enhances proliferation of astrocytes and GFAP expression

EGF stimulates proliferation of astrocytes and transforms quiescent astrocytes into reactive astrocytes (Gonzalez-Perez and Quinones-Hinojosa 2010; Liu et al. 2006; Mayer et al. 2009). GFAP and vimentin are intermediate filament of astrocytes and both are upregulated in astrogliosis (Eliasson et al. 1999). Therefore, we compared GFAP and vimentin expression between 3 sets of rabbit pups—glycerol controls without IVH, vehicle- and rhEGF-treated pups with IVH—at D 14. Immunolabeling revealed that the majority of astrocytes in the corona radiata were unbranched processes running almost parallel to each other in pups without IVH (Fig. 6A). In contrast, periventricular white matter of pups with IVH showed abundance of hypertrophic astrocytes, which exhibit large cell body and multiple processes. There was no significant difference in the morphology of $GFAP^+$ astrocytes between vehicle- and rhEGF-treated pups with IVH. Both stereological quantification of GFAP labeled images and Western blot analyses showed that GFAP expression was higher in pups with IVH compared to controls without IVH ($P< 0.04$ and 0.05, respectively; Fig. 6A, 6B). However, rhEGF treatment did not affect GFAP expression I pups with IVH. Similar to GFAP, vimentin expression was higher in pups with IVH compared to controls without IVH ($P< 0.05$; Fig. 6B); and rhEGF treatment did not significantly affect the levels of vimentin in pups with IVH at D14. Together, IVH increases the expression of GFAP and vimentin at D14, however rhEGF treatment does not further increase their expression.

We next evaluated the effect of rhEGF on GFAP and vimentin expression in pups with IVH at D3. We found that GFAP protein expression was higher in pups with IVH compared to glycerol controls without IVH ($P <0.001$, Fig. 6C). More importantly, GFAP levels were higher in rhEGF-treated compared to vehicle-treated pups with IVH ($P <0.025$). Accordingly, rhEGF treatment enhanced GFAP mRNA expression in pups with IVH relative to vehicle controls at D7 ($P=0.005$, Fig. 6D), but not at D3. We next measured vimentin

Author Manuscript Author Manuscript Author Manuscript Author Manuscript

levels in the three sets of pups. We noted that the onset of IVH did not affect vimentin protein levels at D3, but rhEGF treatment increased expression of vimentin in pups with IVH ($P< 0.034$). In contrast to vimentin protein levels, vimentin mRNA expression was not affected by rhEGF treatment at D3 or 7 (Fig. 6D). This discrepancy between protein and gene expression of vimentin might be attributed to a rapid vimentin mRNA turnover. Together, rhEGF treatment increased GFAP and vimentin expression at D 3 in pups with IVH, but not at D14. A lack of effect of rhEGF treatment on GFAP and vimentin expression at D14 could be because the rabbits received the last dose of rhEGF at D6 and thus, the effect of rhEGF on astrocytes might have diminished by D14.

rhEGF treatment favors astrocytic proliferation, upregulates SOX9, and inhibits Notch signaling

To elucidate the mechanism of rhEGF induced elevation in GFAP in pups with IVH, we assessed the effect of IVH on astrocyte proliferation. S-100β is a calcium binding protein and is specific for astrocytes (Hachem et al. 2005). Thus, we double-labelled the brain sections with S-100β and Ki67 specific antibodies. We found that the development of IVH reduced the density of both total and cycling S-100β$^+$ astrocytes ($P<0.001$ both), and that rhEGF treatment expanded the population of both the total and proliferating astrocytes ($P<0.05$ and 0.007, respectively, Fig. 7A).

Gliogenic switch—a transition from neurogenesis to gliogenesis—is in process in fetal brain in later pregnancy and is regulated by Sox9 and NFIA transcription factors (Kang et al. 2012). As these transcription factors might contribute to astrocytic proliferation and gliosis, we quantified Sox9 and NFIA by RT-qPCR and Western blot analyses. We found that IVH did not affect protein and gene expression of Sox9 or NFIA at D3. However, rhEGF treatment increased Sox9 protein levels at D3 ($P=0.006$, Fig. 7B), but not NFIA. Accordingly, Sox9 mRNA accumulation was higher in rhEGF treated pups relative to vehicle controls at D 7 ($P =0.046$) and displayed a trend toward similar increase at D3 ($P=0.061$, Fig. 7C).

Since Sox9 is implicated in Notch-mediated gliosis and as Sox9 expression is upregulated following Notch activation in embryonic stem cells (Meier-Stiegen et al. 2010; Taylor et al. 2007), we assessed Notch signaling in rabbits treated with rhEGF. We found that rhEGF treatment reduced the release of Notch intracellular domain (NICD) and expression of Hes5 at D3 ($P<0.05$ both, Fig. 7B). Accordingly, Hes5 mRNA expression was lower in rhEGF treated pups with IVH compared to vehicle controls with IVH ($P<0.05$).

Together, rhEGF treatment promotes astrocyte multiplication and elevates SOX9 transcription factors, but suppresses Notch signaling. This suggests that EGF-induced Sox9 upregulation is not related to Notch signaling.

rhEGF treatment induces proliferation of Sox2$^+$ neural cells and does not attenuate Dlx1, Mash1

The high mobility group (HMG) family transcription factor Sox9 is vital for the induction and maintenance of neural stem cell pool in the central nervous system and it is also the master regulator that defines glial fate choice by mediating the neurogenic-to-gliogenic fate

Author Manuscript Author Manuscript Author Manuscript Author Manuscript

switch (Stolt et al. 2003; Vong et al. 2015). Therefore, we evaluated neural progenitor $Sox2^+$ cell in the medial GE and the ventral transcription factors, Dlx1 and Mash1, regulating interneuron neurogenesis.

Sox2 and Ki67 double labeling showed that both proliferating Sox2 cells were reduced in rabbits with IVH compared to controls without IVH ($P<0.05$, Fig. 8A). More importantly, rhEGF treatment increased both total and proliferating $Sox2^+$ cells in pups with IVH ($P<0.05$ both). Reduced density of total and proliferating $Sox2^+$ progenitors can be attributed to suppressed EGF levels in pups with IVH, and accordingly, EGF administration restored Sox2 proliferation and density.

We next assessed Dlx1 and Mash1 transcription factors and found them to be comparable between glycerol controls without IVH, vehicle and rhEGF treated pups with IVH (Fig. 8B). This suggests that rhEGF may not significantly affect interneuron neurogenesis and that increased oligodendrogenesis on rhEGF treatment is perhaps not at the expense of interneuron neurogenesis.

Discussion

IVH is a major complication of prematurity, which affects about 12,000 premature infants every year in the USA. As survival rates of preterm infants have markedly increased, cerebral palsy and cognitive deficits associated with IVH have emerged as major public health concerns. Unfortunately, there is no viable preventive or therapeutic strategy to alleviate IVH-induced complications in survivors with IVH. In the present study, we showed that the development of IVH reduces EGF expression in both rabbits and humans and accordingly, EGF treatment restores OPC maturation, myelination, and clinical recovery in rabbits with IVH. rhEGF treatment inhibited Notch signaling, which possibly contributed to OPC maturation. EGF treatment also exacerbated astrogliosis by driving astroglial proliferation, elevating Sox9 expression, and promoting GFAP transcription in pups with IVH. In addition, EGF treatment increased total and proliferating $Sox2^+$ progenitor pool, which seemingly contributed to both astrogenesis and oligodendrogenesis.

The most novel and clinically relevant finding of this study was that rhEGF treatment enhanced OPC maturation and preserved myelin in a rabbit model of IVH. To our knowledge, this is the first study demonstrating preservation of myelin and improvement in neurologic function with rhEGF treatment in an animal model of IVH. However, role of rhEGF in myelination has been studied in both healthy animals and several animal models of brain injury. A number of studies have shown that EGF is a potent mitogen, which stimulates OPC proliferation, migration, and maturation (Aguirre et al. 2007; Gonzalez-Perez and Quinones-Hinojosa 2010). Indeed, EGFR overexpression in a transgenic mouse model promotes proliferation of OPC progenitors and induces remyelination in an adult model of lysolecithin-induced demyelination (Aguirre et al. 2007). Moreover, intranasal delivery of HB-EGF mobilizes progenitors of SVZ towards demyelinating lesion in the corpus callosum to restore myelination (Cantarella et al. 2008). Similarly, in a neonatal model of chronic hypoxia, intranasal HB-EGF has promoted survival, proliferation, and maturation of OPC as well as neurological recovery (Scafidi et al. 2014). Other than the

Author Manuscript Author Manuscript Author Manuscript Author Manuscript

effect of EGF on OPCs, EGF treatment also increases proliferation of neural cells in the hippocampus and intracerebroventricular infusion of EGF for 7 days in an adult model of traumatic brain injury has led to improvement in cognitive function (Sun et al. 2010). This indicates that EGF might act as a neuroprotectant to preserve both axon and myelin. Together, improvement in myelination and neurologic recovery after rhEGF treatment in a number of previous studies reinforces our finding that the rhEGF treatment promotes OPC maturation and preserves myelin after IVH.

We demonstrated that rhEGF treatment exacerbated astrogliosis in rabbits with IVH; and we also dissected the underlying mechanisms. Specifically, we found that rhEGF treatment increased proliferation of $S100\beta^+$ astrocytes, elevated GFAP and vimentin protein levels, and enhanced transcription of GFAP. Consistent with the present study, previous works have shown that EGFR activation is an upstream signal that induces astrogliosis by driving proliferation of astrocytes, increasing GFAP levels, and converting quiescent astrocytes into reactive astrocytes (Liu et al. 2006; Liu and Neufeld 2007). Accordingly, EGF inhibition has reduced astrogliosis in spinal cord injury model in adult rats (Li et al. 2014). Culture studies on adult neural stem cells from the SVZ of the lateral ventricular wall have revealed that EGF treatment induces proliferation and migration of $GFAP^+$ type-B astrocytes and that upon EGF withdrawal, EGF-stimulated cells differentiate into $O4^+$ oligodendrocytes (Gonzalez-Perez and Quinones-Hinojosa 2010). By contrast, studies in 2D and Bioactive3D culture systems have shown that HB-EGF reduced GFAP mRNA expression and did not affect GFAP and vimentin protein levels (Puschmann et al. 2014). A lack of EGF effect on GFAP expression in this 3D culture study might be attributed to a low dose of EGF used and difference in the culture conditions. In the present study, we observed that rhEGF treatment increased $GFAP^+$ astrocytosis at both D3 and 7, but not at D14. A failure of upsurge in GFAP levels upon rhEGF treatment at D14 might be because the pups received the last dose of rhEGF at D6 and thus, the rhEGF effect diminished by D14. Together, rhEGF treatment led to astrogliosis by enhancing astrocytic proliferation and upregulating GFAP transcription as well as translation.

NFIA and Sox9 are the key transcription factors that regulate embryonic gliogenesis and astrocyogenesis (Kang et al. 2012; Meier-Stiegen et al. 2010; Molofsky and Deneen 2015). Recent studies have shown that Sox9 control gliogenesis by NFIA induction and by its association with NFIA (Stolt et al. 2003). In the present study, we found that rhEGF treatment increased both gene and protein expression of Sox9 in pups with IVH, but not of NFIA. Sox9 gene is regulated by both Sonic hedgehog and Notch signaling. Sox9 enhances cell proliferation and maintains multi-potentiality of neural stem cell both *in vivo* and *in vitro* (Martini et al. 2013; Scott et al. 2010; Swartling et al. 2009). Therefore, elevation in Sox9 levels after rhEGF treatment might have induced proliferative astrocytosis (Fig. 7A) in rabbits with IVH.

We found that both EGF and EGFR were abundantly expressed in the GE relative to other brain regions. Although the onset of IVH reduced EGF expression in the GE, EGFR levels remain unchanged in both humans in rabbits. Changes in the levels of EGF were limited to the GE, but not to the other brain region. This might be because GE is close to the site of hemorrhage, while cortex and white matter are distant from the ventricle. EGF and EGFR

Author Manuscript Author Manuscript Author Manuscript Author Manuscript

expression have been evaluated in neonatal and adult models of brain injury. Hypoxia in P11 rats, which was initiated at P3 led to an increase in EGF expression in mice (Scafidi et al. 2014). Moreover, HB EGF levels are also increased in rats with hypoxia-ischemia (Tanaka et al. 1999). In human patient of multiple sclerosis, HB-EGF immunoreactivity is increased on reactive astrocytes in the active lesion and in the rim around chronic active lesions compared to normal white matter (Schenk et al. 2013). Likewise, neuritic plaques from patients with pathologically confirmed Alzheimer's disease show intense EGFR immunoreactivity (Birecree et al. 1988). Traumatic brain injury results in increased numbers of $GFAP^+/EGFR^+$ stem cells through the dedifferentiation of progenitor cells (Sun et al. 2010). Interestingly, plasma EGF is considered a biomarker for progression to cognitive impairment in PD. Together, EGF and EGFR are associated with brain injury paradigms and their expression is elevated in brain lesions in several brain injury conditions, but by contrast EGF levels are reduced in both rabbits and infants with IVH. We speculate that low EGF levels in IVH diminished the density and proliferation of $Sox2^+$, Olig2, and PDGFRα cells.

EGF treatment preserved myelin and promoted clinical recovery in our animal model of IVH and in models of demyelination as well as chronic hypoxia (Aguirre and Gallo 2007; Aguirre et al. 2005; Scafidi et al. 2014). By contrast, EGF inhibition using anti-EGF antibody alleviates experimental autoimmune encephalomyelitis by inducing oligodendrogenesis and neurogenesis at expense of astrogenesis (Amir-Levy et al. 2014). Thus, rhEGF enhancing myelination in models of brain injury is context-dependent and specific to experimental conditions. EGF treatment can also induce neurotoxicities, including apoptosis, oxidative neural cell death, and reduced cell maturation (Cha et al. 2000; Hognason et al. 2001). Even though EGF is a mitogen, it does not initiate malignant transformation. However, EGF might promote tumors and thus, investigators have raised doubts on its clinical use despite concrete demonstrations of efficacy in experimental conditions (Berlanga-Acosta et al. 2009). Intranasal EGF has been successfully used in a rodent model of chronic hypoxia to enhance myelination (Scafidi et al. 2014), and intranasal route is convenient mode of drug administration, which may be tried in infants with IVH. Together, the safety and efficacy of EGF treatment needs confirmation in infants with IVH by performing a randomized controlled clinical trial.

In conclusion, we show that rhEGF promotes proliferation and maturation of OPCs, preserves myelin, and hastens neurological recovery in rabbits with IVH. Since rhEGF treatment inhibits Notch signaling, downregulation of Notch pathways conceivably contributes to OPC maturation in rhEGF treated pups with IVH. rhEGF treatment exacerbates astrogliosis by inducing astroglial proliferation, elevating Sox9 expression, and promoting GFAP transcription in pups with IVH. If rhEGF treatment demonstrates safety and efficacy in ameliorating white matter injury in premature infants with IVH, this will improve the neurologic outcome of premature infants with IVH.

Acknowledgments

This work was supported by NIH–NINDS Grants RO1 NS071263 (PB) and R01NS083947 (PB). We thank Joanne Abrahams for the assistance with images.

Author Manuscript Author Manuscript Author Manuscript Author Manuscript

References

Aguirre A, Dupree JL, Mangin JM, Gallo V. A functional role for EGFR signaling in myelination and remyelination. Nat Neurosci. 2007; 10:990–1002. [PubMed: 17618276]

Aguirre A, Gallo V. Reduced EGFR signaling in progenitor cells of the adult subventricular zone attenuates oligodendrogenesis after demyelination. Neuron Glia Biol. 2007; 3:209–20. [PubMed: 18634612]

Aguirre A, Rizvi TA, Ratner N, Gallo V. Overexpression of the epidermal growth factor receptor confers migratory properties to nonmigratory postnatal neural progenitors. J Neurosci. 2005; 25:11092–106. [PubMed: 16319309]

Amir-Levy Y, Mausner-Fainberg K, Karni A. Treatment with Anti-EGF Ab Ameliorates Experimental Autoimmune Encephalomyelitis via Induction of Neurogenesis and Oligodendrogenesis. Mult Scler Int. 2014; 2014:926134. [PubMed: 25610650]

Ballabh P. Pathogenesis and prevention of intraventricular hemorrhage. Clin Perinatol. 2014; 41:47–67. [PubMed: 24524446]

Ballabh P, Xu H, Hu F, Braun A, Smith K, Rivera A, Lou N, Ungvari Z, Goldman SA, Csiszar A, et al. Angiogenic inhibition reduces germinal matrix hemorrhage. Nat Med. 2007; 13:477–85. [PubMed: 17401377]

Berlanga-Acosta J, Gavilondo-Cowley J, Lopez-Saura P, Gonzalez-Lopez T, Castro-Santana MD, Lopez-Mola E, Guillen-Nieto G, Herrera-Martinez L. Epidermal growth factor in clinical practice - a review of its biological actions, clinical indications and safety implications. Int Wound J. 2009; 6:331–46. [PubMed: 19912390]

Birecree E, Whetsell WO Jr, Stoscheck C, King LE Jr, Nanney LB. Immunoreactive epidermal growth factor receptors in neuritic plaques from patients with Alzheimer's disease. J Neuropathol Exp Neurol. 1988; 47:549–60. [PubMed: 3049945]

Bystron I, Blakemore C, Rakic P. Development of the human cerebral cortex: Boulder Committee revisited. Nat Rev Neurosci. 2008; 9:110–22. [PubMed: 18209730]

Cantarella C, Cayre M, Magalon K, Durbec P. Intranasal HB-EGF administration favors adult SVZ cell mobilization to demyelinated lesions in mouse corpus callosum. Dev Neurobiol. 2008; 68:223–36. [PubMed: 18000828]

Cha YK, Kim YH, Ahn YH, Koh JY. Epidermal growth factor induces oxidative neuronal injury in cortical culture. J Neurochem. 2000; 75:298–303. [PubMed: 10854274]

Chua CO, Chahboune H, Braun A, Dummula K, Chua CE, Yu J, Ungvari Z, Sherbany AA, Hyder F, Ballabh P. Consequences of intraventricular hemorrhage in a rabbit pup model. Stroke. 2009; 40:3369–77. [PubMed: 19661479]

Doetsch F, Petreanu L, Caille I, Garcia-Verdugo JM, Alvarez-Buylla A. EGF converts transit-amplifying neurogenic precursors in the adult brain into multipotent stem cells. Neuron. 2002; 36:1021–34. [PubMed: 12495619]

Dummula K, Vinukonda G, Chu P, Xing Y, Hu F, Mailk S, Csiszar A, Chua C, Mouton P, Kayton RJ, et al. Bone morphogenetic protein inhibition promotes neurological recovery after intraventricular hemorrhage. J Neurosci. 2011; 31:12068–82. [PubMed: 21865450]

Eliasson C, Sahlgren C, Berthold CH, Stakeberg J, Celis JE, Betsholtz C, Eriksson JE, Pekny M. Intermediate filament protein partnership in astrocytes. J Biol Chem. 1999; 274:23996–4006. [PubMed: 10446168]

Flores AI, Narayanan SP, Morse EN, Shick HE, Yin X, Kidd G, Avila RL, Kirschner DA, Macklin WB. Constitutively active Akt induces enhanced myelination in the CNS. J Neurosci. 2008; 28:7174–83. [PubMed: 18614687]

Galvez-Contreras AY, Quinones-Hinojosa A, Gonzalez-Perez O. The role of EGFR and ErbB family related proteins in the oligodendrocyte specification in germinal niches of the adult mammalian brain. Front Cell Neurosci. 2013; 7:258. [PubMed: 24381541]

Gonzalez-Perez O, Alvarez-Buylla A. Oligodendrogenesis in the subventricular zone and the role of epidermal growth factor. Brain Res Rev. 2011; 67:147–56. [PubMed: 21236296]

Author Manuscript Author Manuscript Author Manuscript Author Manuscript

Gonzalez-Perez O, Quinones-Hinojosa A. Dose-dependent effect of EGF on migration and differentiation of adult subventricular zone astrocytes. Glia. 2010; 58:975–83. [PubMed: 20187143]

Gonzalez-Perez O, Romero-Rodriguez R, Soriano-Navarro M, Garcia-Verdugo JM, Alvarez-Buylla A. Epidermal growth factor induces the progeny of subventricular zone type B cells to migrate and differentiate into oligodendrocytes. Stem Cells. 2009; 27:2032–43. [PubMed: 19544429]

Guardiola-Diaz HM, Ishii A, Bansal R. Erk1/2 MAPK and mTOR signaling sequentially regulates progression through distinct stages of oligodendrocyte differentiation. Glia. 2012; 60:476–86. [PubMed: 22144101]

Hachem S, Aguirre A, Vives V, Marks A, Gallo V, Legraverend C. Spatial and temporal expression of S100B in cells of oligodendrocyte lineage. Glia. 2005; 51:81–97. [PubMed: 15782413]

Herrmann JE, Imura T, Song B, Qi J, Ao Y, Nguyen TK, Korsak RA, Takeda K, Akira S, Sofroniew MV. STAT3 is a critical regulator of astrogliosis and scar formation after spinal cord injury. J Neurosci. 2008; 28:7231–43. [PubMed: 18614693]

Hognason T, Chatterjee S, Vartanian T, Ratan RR, Ernewein KM, Habib AA. Epidermal growth factor receptor induced apoptosis: potentiation by inhibition of Ras signaling. FEBS Lett. 2001; 491:9–15. [PubMed: 11226409]

Jorissen RN, Walker F, Pouliot N, Garrett TP, Ward CW, Burgess AW. Epidermal growth factor receptor: mechanisms of activation and signalling. Exp Cell Res. 2003; 284:31–53. [PubMed: 12648464]

Kang P, Lee HK, Glasgow SM, Finley M, Donti T, Gaber ZB, Graham BH, Foster AE, Novitch BG, Gronostajski RM, et al. Sox9 and NFIA coordinate a transcriptional regulatory cascade during the initiation of gliogenesis. Neuron. 2012; 74:79–94. [PubMed: 22500632]

Kessaris N, Fogarty M, Iannarelli P, Grist M, Wegner M, Richardson WD. Competing waves of oligodendrocytes in the forebrain and postnatal elimination of an embryonic lineage. Nat Neurosci. 2006; 9:173–9. [PubMed: 16388308]

Kuhn HG, Winkler J, Kempermann G, Thal LJ, Gage FH. Epidermal growth factor and fibroblast growth factor-2 have different effects on neural progenitors in the adult rat brain. J Neurosci. 1997; 17:5820–9. [PubMed: 9221780]

Li ZW, Li JJ, Wang L, Zhang JP, Wu JJ, Mao XQ, Shi GF, Wang Q, Wang F, Zou J. Epidermal growth factor receptor inhibitor ameliorates excessive astrogliosis and improves the regeneration microenvironment and functional recovery in adult rats following spinal cord injury. J Neuroinflammation. 2014; 11:71. [PubMed: 24708754]

Liu B, Chen H, Johns TG, Neufeld AH. Epidermal growth factor receptor activation: an upstream signal for transition of quiescent astrocytes into reactive astrocytes after neural injury. J Neurosci. 2006; 26:7532–40. [PubMed: 16837601]

Liu B, Neufeld AH. Activation of epidermal growth factor receptors in astrocytes: from development to neural injury. J Neurosci Res. 2007; 85:3523–9. [PubMed: 17526018]

Martini S, Bernoth K, Main H, Ortega GD, Lendahl U, Just U, Schwanbeck R. A critical role for Sox9 in notch-induced astrogliogenesis and stem cell maintenance. Stem Cells. 2013; 31:741–51. [PubMed: 23307615]

Mayer SI, Rossler OG, Endo T, Charnay P, Thiel G. Epidermal-growth-factor-induced proliferation of astrocytes requires Egr transcription factors. J Cell Sci. 2009; 122:3340–50. [PubMed: 19706684]

Meier-Stiegen F, Schwanbeck R, Bernoth K, Martini S, Hieronymus T, Ruau D, Zenke M, Just U. Activated Notch1 target genes during embryonic cell differentiation depend on the cellular context and include lineage determinants and inhibitors. PLoS One. 2010; 5:e11481. [PubMed: 20628604]

Molofsky AV, Deneen B. Astrocyte development: A Guide for the Perplexed. Glia. 2015; 63:1320–9. [PubMed: 25963996]

Mouton PR, Chachich ME, Quigley C, Spangler E, Ingram DK. Caloric restriction attenuates amyloid deposition in middle-aged dtg APP/PS1 mice. Neurosci Lett. 2009; 464:184–7. [PubMed: 19699265]

Narayanan SP, Flores AI, Wang F, Macklin WB. Akt signals through the mammalian target of rapamycin pathway to regulate CNS myelination. J Neurosci. 2009; 29:6860–70. [PubMed: 19474313]

Author Manuscript Author Manuscript Author Manuscript Author Manuscript

Puschmann TB, Zanden C, Lebkuechner I, Philippot C, de Pablo Y, Liu J, Pekny M. HB-EGF affects astrocyte morphology, proliferation, differentiation, and the expression of intermediate filament proteins. J Neurochem. 2014; 128:878–89. [PubMed: 24188029]

Scafidi J, Hammond TR, Scafidi S, Ritter J, Jablonska B, Roncal M, Szigeti-Buck K, Coman D, Huang Y, McCarter RJ Jr, et al. Intranasal epidermal growth factor treatment rescues neonatal brain injury. Nature. 2014; 506:230–4. [PubMed: 24390343]

Schenk GJ, Dijkstra S, van het Hof AJ, van der Pol SM, Drexhage JA, van der Valk P, Reijerkerk A, van Horssen J, de Vries HE. Roles for HB-EGF and CD9 in multiple sclerosis. Glia. 2013; 61:1890–905. [PubMed: 24038577]

Scott CE, Wynn SL, Sesay A, Cruz C, Cheung M, Gomez Gaviro MV, Booth S, Gao B, Cheah KS, Lovell-Badge R, et al. SOX9 induces and maintains neural stem cells. Nat Neurosci. 2010; 13:1181–9. [PubMed: 20871603]

Stolt CC, Lommes P, Sock E, Chaboissier MC, Schedl A, Wegner M. The Sox9 transcription factor determines glial fate choice in the developing spinal cord. Genes Dev. 2003; 17:1677–89. [PubMed: 12842915]

Sun D, Bullock MR, Altememi N, Zhou Z, Hagood S, Rolfe A, McGinn MJ, Hamm R, Colello RJ. The effect of epidermal growth factor in the injured brain after trauma in rats. J Neurotrauma. 2010; 27:923–38. [PubMed: 20158379]

Sun Y, Lehmbecker A, Kalkuhl A, Deschl U, Sun W, Rohn K, Tzvetanova ID, Nave KA, Baumgartner W, Ulrich R. STAT3 represents a molecular switch possibly inducing astroglial instead of oligodendroglial differentiation of oligodendroglial progenitor cells in Theiler's murine encephalomyelitis. Neuropathol Appl Neurobiol. 2015; 41:347–70. [PubMed: 24606160]

Swartling FJ, Ferletta M, Kastemar M, Weiss WA, Westermark B. Cyclic GMP-dependent protein kinase II inhibits cell proliferation, Sox9 expression and Akt phosphorylation in human glioma cell lines. Oncogene. 2009; 28:3121–31. [PubMed: 19543319]

Tanaka N, Sasahara M, Ohno M, Higashiyama S, Hayase Y, Shimada M. Heparin-binding epidermal growth factor-like growth factor mRNA expression in neonatal rat brain with hypoxic/ischemic injury. Brain Res. 1999; 827:130–8. [PubMed: 10320701]

Taylor MK, Yeager K, Morrison SJ. Physiological Notch signaling promotes gliogenesis in the developing peripheral and central nervous systems. Development. 2007; 134:2435–47. [PubMed: 17537790]

Tyler WA, Jain MR, Cifelli SE, Li Q, Ku L, Feng Y, Li H, Wood TL. Proteomic identification of novel targets regulated by the mammalian target of rapamycin pathway during oligodendrocyte differentiation. Glia. 2011; 59:1754–69. [PubMed: 21858874]

Vinukonda G, Csiszar A, Hu F, Dummula K, Pandey NK, Zia MT, Ferreri NR, Ungvari Z, LaGamma EF, Ballabh P. Neuroprotection in a rabbit model of intraventricular haemorrhage by cyclooxygenase-2, prostanoid receptor-1 or tumour necrosis factor-alpha inhibition. Brain. 2010; 133:2264–80. [PubMed: 20488889]

Vong KI, Leung CK, Behringer RR, Kwan KM. Sox9 is critical for suppression of neurogenesis but not initiation of gliogenesis in the cerebellum. Mol Brain. 2015; 8:25. [PubMed: 25888505]

Author Manuscript Author Manuscript Author Manuscript Author Manuscript

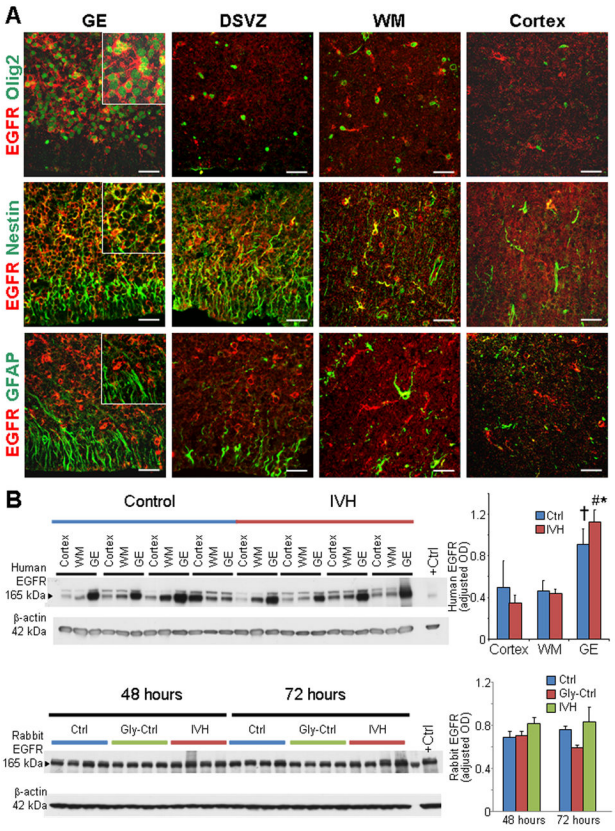

Fig. 1. Human ganglionic eminence exhibits abundance of EGFR; and IVH does not affect EGFR expression

A) Representative immunofluorescence of cryosections from 23 gw infant, which was labeled using EGFR with Olig2, (upper panel), nestin (middle panel), or GFAP (lower panel) specific antibody. EGFR was abundantly expressed on Olig2$^+$ and nestin$^+$ precursor cells of the medial GE and white matter. GFAP$^+$ radial glia in the GE and astrocytes in the embryonic whiter matter (WM) weakly expressed EGFR. Scale bar, 20 μm. **B)** Western blot analyses were performed for EGFR on homogenates made from tissues taken from the cortical plate (cortex), WM, and GE of preterm infants with and without IVH, as indicated. The bar charts are mean ± s.e.m. (n = 6 each). Values were normalized to β actin levels. EGFR expression was significantly higher in the GE compared to the cortical plate and WM of infants with IVH. In infants without IVH, EGFR levels were elevated in the GE compared to the white matter, but not to the cortex. EGFR expression was comparable between infants with and without IVH for the three brain regions. **P<0.01 GE vs. WM, # P<0.01 GE vs. cortex in infants with IVH; †P<0.05 GE vs. WM in infants without IVH. **C)** Western blot analyses for EGFR was performed on lysates made from the forebrain slices of rabbit pups with and without IVH at 48 and 72 h age. Bar chart shows mean ± s.e.m. (n=5 each group). EGFR protein levels were comparable between pups with and without IVH. DSVZ, dorsal cortical subventricular zone.

Author Manuscript Author Manuscript Author Manuscript Author Manuscript

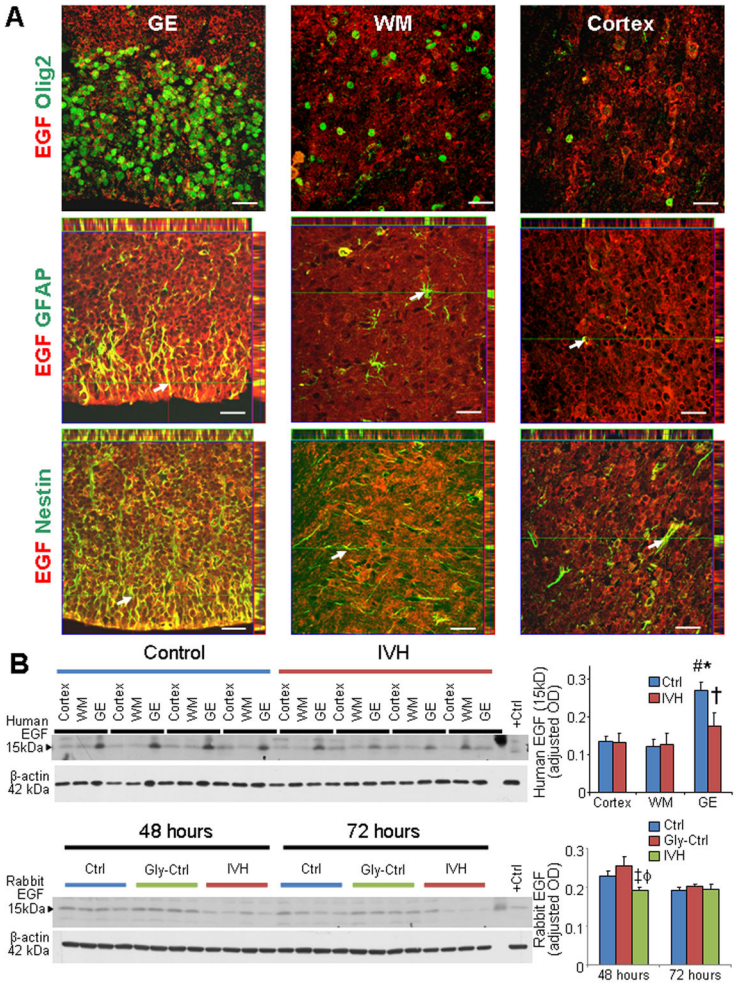

Fig. 2. EGF expression was reduced in both rabbits and humans with IVH

A) Representative immunofluorescence of cryosections from 23 gw infant double labeled with EGF and Olig2 (upper panel), GFAP (middle panel), or nestin (lower panel) antibodies. For middle and lower panel, above and to the right of images are orthogonal views in x–z and y–z planes of a composite z-stalk of a series of confocal images taken 0.4 μm apart. Arrow shows co-localization of EGF and GFAP/nestin expression in the GE. Note that EGF is abundantly expressed on $GFAP^+$ and $nestin^+$ radial glia of the medial GE and dorsal cortical SVZ. Expression of EGF was weak-to-absent on $Olig2^+$ cells. EGF immunoreactivity is more intense in the GE relative to the WM. Scale bar, 20 μm. **B)** Representative Western blot analyses for EGF on homogenates made from tissues taken from cortex, WM, and GE of preterm infants with and without IVH, as indicated. The bar charts are mean ± s.e.m. (n = 6 each). Values were normalized to β actin levels. Note higher EGF expression (15kDa) in the GE relative to the cortex and WM in infants without IVH and reduced EGF levels in the GE of infants with IVH compared to controls without IVH. **C)** Western blot analyses for EGF were performed on lysates made from forebrain slices of rabbit pups with IVH and without IVH at 48 and 72 h age. Bar chart shows mean ± s.e.m. (n=5 each group). EGF protein levels were lower in pups with IVH compared to pups without IVH at 48h. *P<0.01 GE vs. WM; # P<0.01 GE vs. cortex; †P<0.05 IVH vs. no IVH

in the GE; ‡P<0.05 for IVH vs. untreated no IVH controls; ϕP<0.01 for IVH vs. glycerol treated controls.

Author Manuscript Author Manuscript Author Manuscript Author Manuscript

Author Manuscript Author Manuscript Author Manuscript Author Manuscript

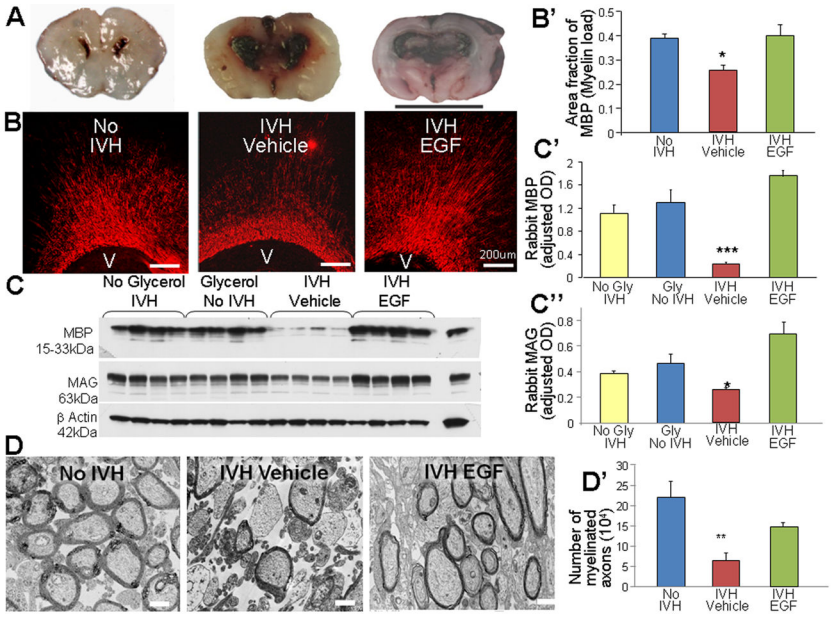

Fig. 3. EGF treatment preserves myelin in rabbits with IVH

A) Coronal brain slice from frontal lobe of E29 rabbit pup show normal slit-like ventricle (left panel), moderate hemorrhage in the ventricle (middle panel) and severe hemorrhage (right panel) resulting in fusion of the two ventricles (bottom panel). Scale bar, 1 cm. **B, B′**) Representative immunofluorescence of myelin basic protein (MBP) in the corona radiata of D14 pups. Data are mean ± s.e.m. (n = 5 each group). Volume fractions of MBP were higher in the corpus callosum and corona radiata of EGF-treated pups compared with vehicle controls with IVH. Scale bar, 200 μm. V, ventricular side. **C, C′ and C″**) Representative Western blot analysis for MBP and MAG in the forebrain of premature rabbit pups, as indicated, at D14. Adult rat brain was used as positive control. Each lane represents lysate from a whole coronal slice taken at the level of midseptal nucleus of one brain. Bar chart shows mean ± s.e.m. (n=5 each group). MBP and MAG expression were higher in EGF treated pups compared with vehicle treated controls. **D, D′**) Typical electron micrograph from rabbit pups with and without IVH, and pups with IVH treated with rhEGF at D 14. Note that myelinated axons were fewer in pups with IVH compared to controls without IVH and that rhEGF treatment significantly increased the number of myelinated axons in pups with IVH. Scale bar, 1 μm. *P<0.05,**<0.01, ***P<0.001 pups with vs. without IVH. #P<0.05, ###P<0.001 vehicle vs. rhEGF treated pups with IVH.

Author Manuscript Author Manuscript Author Manuscript Author Manuscript

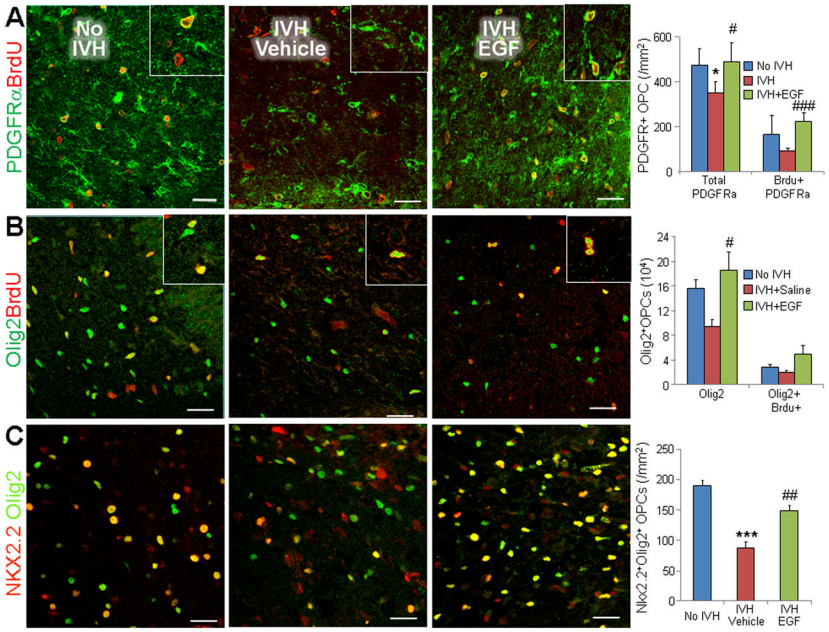

Fig. 4. EGF administration promotes OPC proliferation and maturation

A) Representative immunofluorescence of cryosections from a 3 d old pup double-labeled with PDGFRα and BrdU specific antibodies. Graphs show mean ± SEM (n = 5 each). Cycling PDGFRα+ cells (arrowhead) were reduced in pups with IVH, and rhEGF treatment increased their density**. B)** Representative immunofluorescence of cryosections from a 3 d old pup double-labeled with Olig2 and BrdU specific antibodies. Bar-charts are mean±SEM (n= 5 each). Note total and cycling $Olig2^{+}$ cells show a trend toward reduction in pups with IVH (compared to no IVH controls) and an increase in rhEGF treated pups relative to vehicle controls. Arrowhead indicated $Olig2^{+}BrdU^{+}$ cells. **C)** Cryosections were double labeled with Nkx2.2 and Olig2 antibodies. Graphs show mean±SEM (n=5 each). Note reduced number of cells co-labeled with $Nkx2.2^{+}Olig2^{+}$ (arrowhead) in pups with IVH compared to vehicle controls, and rhEGF treatment increased the number in this subset of cells. *P<0.05, ***P<0.001 pups with vs. without IVH. #P<0.05, ##P<0.01, ###P<0.001 vehicle vs. rhEGF treated pups with IVH. Scale bar, 20μm.

Author Manuscript Author Manuscript Author Manuscript Author Manuscript

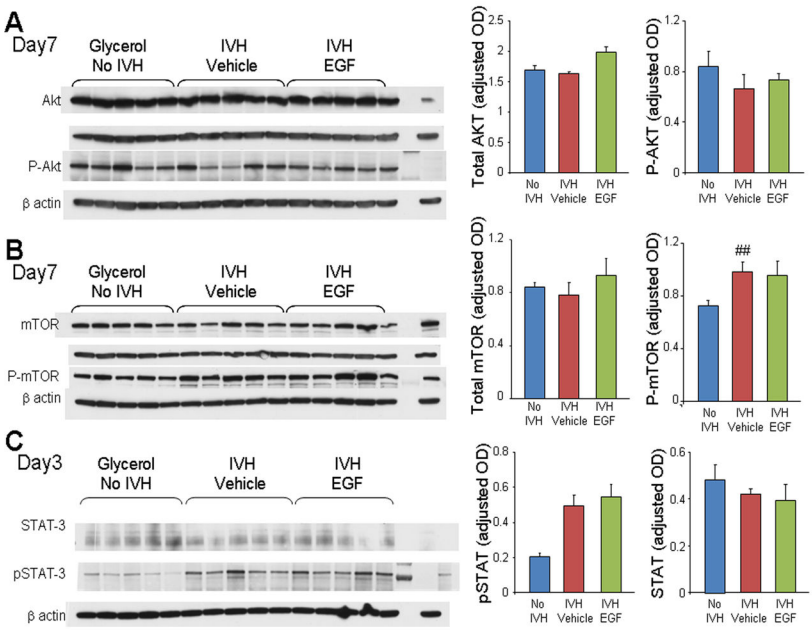

Fig. 5. RhEGF treatment does not affect mTOR, Akt, or STAT-3 signaling

Representative Western blot analyses performed on forebrain homogenates (1 cm slice at mid-septal nucleus) of pups at D3 or 7, as indicated. Adult rat brain was positive-control. Graph shows mean ± s.e.m. (n = 5 each). Values were normalized to β-actin. **A, B, C)** mTOR, Akt, phospho-mTOR, phosphor-Akt and STAT-3 were comparable between controls without IVH, vehicle- and rhEGF-treated pups with IVH. However, P-STAT-3 levels were higher in pups with IVH compared to controls without IVH and rhEGF treatment did not make any difference. **P < 0.01 for no IVH vs. IVH.

Author Manuscript Author Manuscript Author Manuscript Author Manuscript

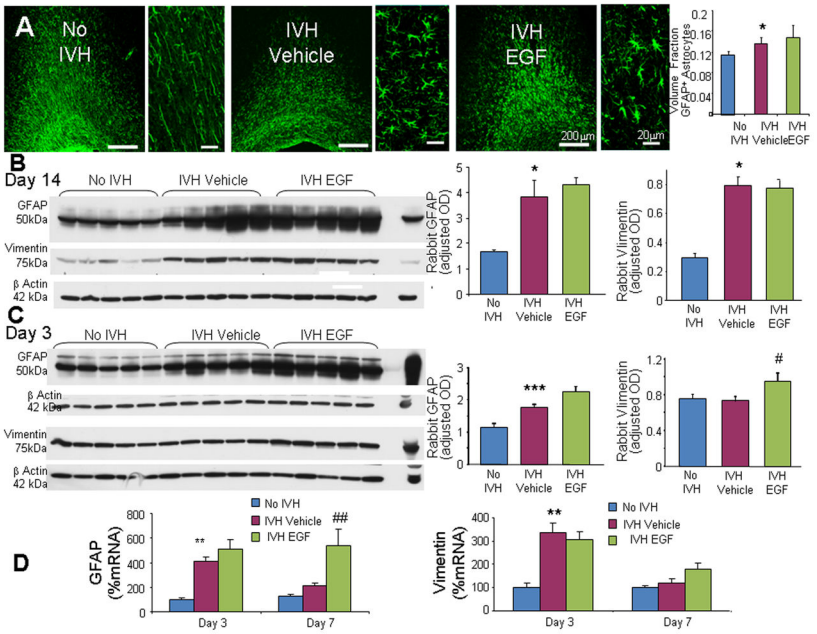

Fig. 6. rhEGF treatment promotes astrogliosis

A) Representative immunofluorescence of cryosections from pups (D14) labeled with GFAP antibody are shown, as indicated. 'V' indicates ventricular side. Rectangular panels are high power view of the adjacent image. Note abundant hypertrophic astrocytes in vehicle and rhEGF treated pups with IVH. Scale bar, 200 μm and 20 μm, as indicated. Graph shows mean ± s.e.m. (n = 5 each). rhEGF treatment did not affect volume fraction of astroglial fibers compared to vehicle controls on stereological-analyses. **B)** Western blot analyses for GFAP and vimentin were performed in forebrain homogenates of pups (D 14). Adult rat brain was positive-control. Graph shows mean ± s.e.m. (n = 5 each). Values were normalized to β-actin. rhEGF treatment did not affect GFAP or vimentin expression in pups with IVH. **C)** Western blot analyses for GFAP and vimentin were performed in forebrain homogenates of pups (D 3). Adult rat brain was positive-control. Graph shows mean ± s.e.m. (n = 5 each). Values were normalized to β-actin. rhEGF treatment increased both GFAP and vimentin expression in pups with IVH. **D)** Data are mean ± s.e.m. GFAP mRNA expression increased with rhEGF treatment at D7, not D3. However, vimentin mRNA expression was not affected by rhEGF treatment at D 3 or 7. *P < 0.05, **P < 0.01, ***P < 0.001 for no IVH vs. IVH. #P < 0.05, ##P < 0.01for vehicle treated vs. rhEGF treated pups with IVH.

Author Manuscript
Author Manuscript
Author Manuscript
Author Manuscript

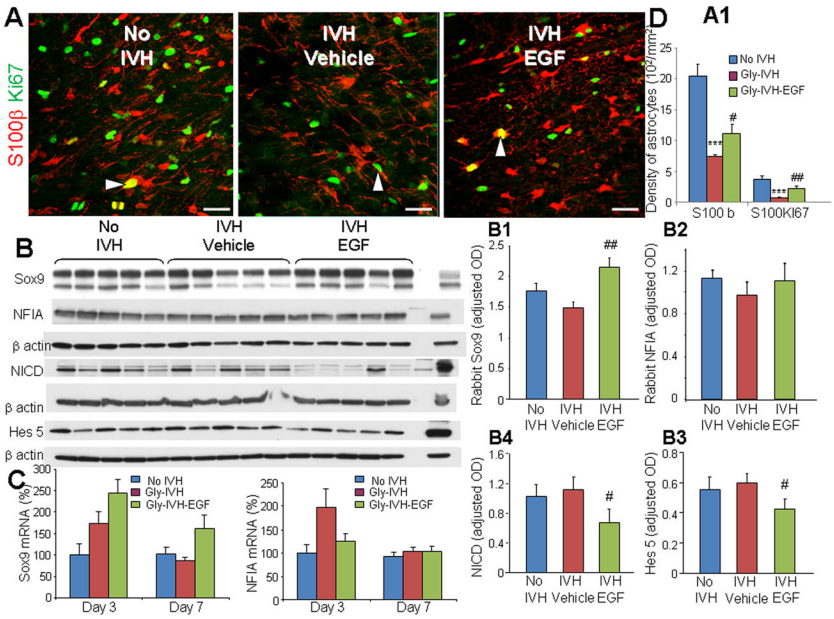

Fig. 7. rhEGF increases astrocytic proliferation, upregulates Sox9 and blocks Notch signaling

A, A1) Representative immunofluorescence of cryosections from pups (D3) labeled with S100β and Ki67 antibodies. Note reduced density of total and proliferating (arrowhead) S100β in pups with IVH and increase in their density on rhEGF treatment. Data are mean ± s.e.m. Scale Bar, 20μm. **B–B4)** Representative Western blot analyses of Sox9, NFIA, NICD, and Hes5 performed in forebrain homogenates of pups at D3. Adult rat brain was positive-control. Graph shows mean ± s.e.m. (n = 5 each). Values were normalized to β-actin. rhEGF treatment increased Sox9 protein levels, reduced NICD and Hes5 expression, and did not change NFIA levels. **C)** Bar Chart shows mean ± s.e.m. (n = 5 each). rhEGF treatment increased Sox9 mRNA accumulation in pups with IVH, but did not affect NFIA mRNA. $P < 0.001$ for no IVH vs. IVH. #$P < 0.05$, ##$P < 0.01$ for vehicle treated vs. rhEGF treated pups with IVH.

Author Manuscript Author Manuscript Author Manuscript Author Manuscript

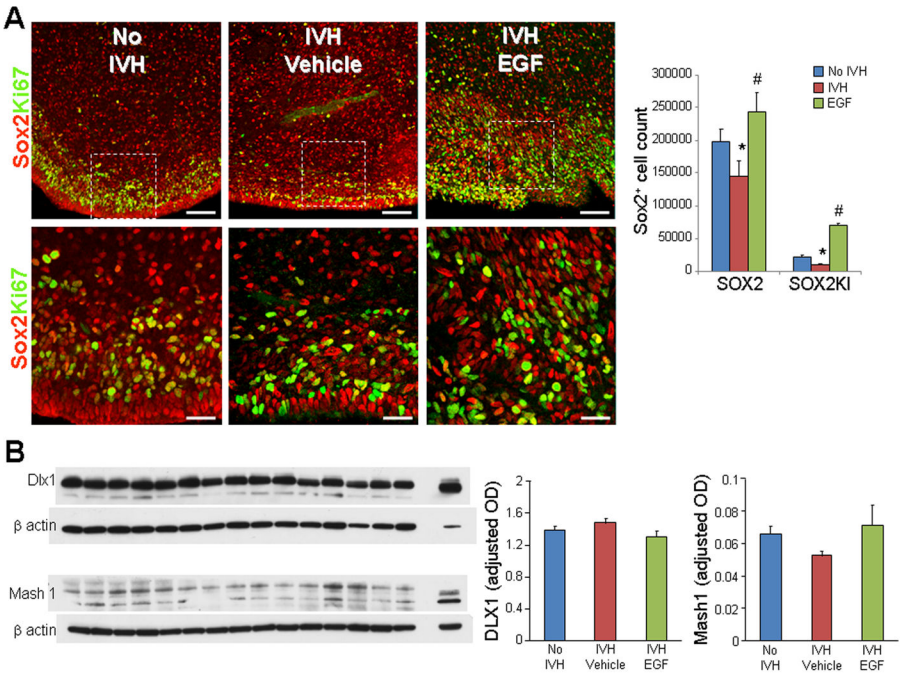

Fig. 8. rhEGF treatment induces proliferation of Sox2$^+$ cells and does not affect Dlx1, Mash1 proteins

A) Representative immunofluorescence of cryosections from pups (D3) labeled with Sox2 and Ki67 antibodies. Lower panels are high magnification images of the boxed area in the upper panel. Note reduced density of total and proliferating (arrowhead) Sox2 in pups with IVH and increase in their density on rhEGF treatment. Data are mean ± s.e.m. Scale Bar, 50 μm (upper panel), 20μm (lower panel). **B)** A typical Western blot analyses of Dlx1, and Mash1 performed on forebrain homogenates of pups at D3. Adult rat brain was positive-control. Graph shows mean ± s.e.m. (n = 5 each). Values were normalized to β-actin. rhEGF treatment did not affect Dlx1 and Mash1 levels. *P < 0.05 for no IVH vs. IVH. #P < 0.05, for vehicle treated vs. rhEGF treated pups with IVH.

Author Manuscript Author Manuscript Author Manuscript Author Manuscript

Table

Neurobehavioral evaluation of rhEGF and vehicle treated pups with IVH and Controls without IVH at postnatal day 14

System	Test	No IVH (n=12)	IVH vehicle (n=10)	IVH, rhEGF (n=9)
Cranial Nerve	Aversive response to alcohol	3 (3,3)	3 (3,3)	3 (3,3)
	Sucking and Swallowing	3 (3,3)	3 (3,3)	3 (3,3)
Motor	**Motor activity**			
	Head	3 (3,3)	3 (3,3)	3 (3,3)
	Fore Legs	3 (3,3)	3 (3,3)	3 (3,3)
	Hind Legs	3 (3,3)	2.5 (1,3)	3 (3,3)
	Righting reflex[a]	5 (5,5)	4 (2,5)[#]	5 (5,5)[*]
	Locomotion on 30° inclination[b]	3 (3,3)	3 (2,3)	3 (3,3)
	Tone[c]: Forelimb	0 (0,0)	0 (0,0)	0 (0,0)
	Tone[c]: Hind Limb	0 (0,0)	0 (0,0)	0 (0,0)
	Inability to hold their position at 60° Inclination for 15 s or more (latency to slip down the slope, if <15s)	0%	40%	11%
	Inability to walk more than 60 inches in one minute (%)	0%	**40%**	**11%**
	Gait[d]	4 (3.5,4)	3 (2,4)	4 (4,4)[*]
	Motor Impairment	0%	**40%**	**11%**
Sensory	Facial touch	3 (3,3)	3 (3,3)	3 (3,3)
	Pain	3 (3,3)	3 (3,3)	3 (3,3)

Values are median and interquartile range. Zero is the worst response and 3 is the best response, unless otherwise noted.

[*] P<0.05 for vehicle treated vs. rhEGF treated pups with IVH

[#] P<0.05, for glycerol treated pups without IVH and vehicle treated pups with IVH

[a] Score (range, 1–5): no. of times turns prone within 2 seconds when placed in supine out of 5 tries.

[b] Score (range, 0–3) 0, does not walk; 1, takes a few steps (less than 8 inches); 2, walks for 9–18 inches; 3, walks very well beyond 18 inches.

[c] Score (range, 1–3): 0, no increase in tone; 1, slight increase in tone; 2, considerable increase in tone; 3, limb rigid in flexion or extension.

[d] Gait was graded as 0 (no locomotion), 1 (crawls with trunk touching the ground for few steps and then rolls over), 2 (walks taking alternate steps, trunk low and cannot walk on inclined surface), 3 (walks taking alternate steps, cannot propel its body using synchronously the hind legs, but walks on 30° inclined surface), 4 (walks, runs, and jumps without restriction, propels the body using synchronously the back legs, but limitation in speed, balance, and coordination manifesting as clumsiness in gait), or 5 (normal walking).

[d] Motor impairment was defined as weakness in either fore- or hind-legs and distance walked ≤60 inches in 60 seconds.